

# A GRID-BASED KINEMATIC DISTRIBUTED HYDROLOGICAL MODEL FOR DIGITAL RIVER BASIN<sup>①</sup>

Jintao Liu, Jie Feng, Martins Y. Otache<sup>②</sup>

<sup>②</sup> State Key Laboratory of Hydrology-Water Resources and Hydraulic Engineering, Hohai University, Nanjing 210098, People's Republic of China, jtliu@hhu.edu.cn

**Abstract** A grid-based kinematic overland flow routing model for rainfall-runoff modeling was developed for flood forecasting. The watershed was sub-divided into a raster system for representing the spatial variability of soil, vegetation and rainfall, etc. In each grid, hydrological processes such as interception, infiltration and overland flow were considered. Runoff generated in each grid was routed by a kinematic wave method according to the digital river basin extracted by using DEM by DigitalHydro software package. The model was applied to Shiguanhe river basin. The model was able to reproduce runoff volume and peak discharge with high efficiency.

**Key words** Grid; DEM; Kinematic wave method; Distributed hydrology model

## 1 INTRODUCTION

A distributed hydrology model is developed and applied to Shiguanhe river basin, an experimental basin during the Intensified Observation Period (I.O.P.) of HUBEX in 1998/1999. The Shiguanhe river basin which always has great impact on peak flow of Huaihe River with an area of 158160 km<sup>2</sup> is located in the Daibie Mountain area. Therefore, it is of particular interest to predict the flood pattern based on the main hydrological mechanisms.

Several flood forecasting models have been applied to the Shiguanhe river basin. Topmodel (Beven, et al., 1984) was used to simulate discharge of Shiguanhe river basin during the summer of 1998 by Liu et al (2002) and the success was limited. Li et al (2004) developed a grid-based Xinanjiang

model to couple weather radar rainfall data into real-time flood forecasting. The Xinanjiang model parameters used in each grid were calibrated by discharge data from Jiangjiayi station with all the grids having the same parameters.

Based on past experiences, the grid-based overland flow routing model for rainfall-runoff modeling is developed. In addition, this model is designed not only to integrate the weather radar rainfall but also to represent the spatial variability of the basin through a square raster system. The raster system is used as the fundamental computation units while all the grids are divided into two groups such as the hillslope and river according to DigitalHydro package.

Based on the background given, the objective of this paper is to develop a distributed hydrology model for rainfall-runoff modeling which includes main mechanisms leading to the runoff generation in the study basin during the flood shaping periods. The spatially varied soils, crops, terrains, rainfall and other hydrological characteristics are considered. The model theory and structure are presented in section 2 and 3 respectively;

<sup>①</sup> This work is supported by the State Key Laboratory of Hydrology-Water Resources and Hydraulic Engineering Open Foundation, Hohai University, China (2006411811) and the Fok Ying-Tong Education Foundation for Young Teachers in the Higher Education Institutions of China (101075).



delineation of digital river basin for Shiguanhe basin is described in section 4 while section 5 describes the calibration and validation of the model.

## 2 KINEMATIC WAVE MODEL

The one-dimensional kinematic wave equation for shallow water flow over a plane is given by:

$$\frac{\partial h}{\partial t} + \alpha \frac{\partial h^m}{\partial x} = q_{lat}(x,t) \quad (1)$$

Here,  $h$  is overland flow depth,  $q_{lat}(x,t)$  is the net inflow including the overland flow section,  $\alpha$  and  $m$  are coefficients. Under the kinematic wave approximation, the discharge is a function of overland flow depth (Kibler, et al., 1970) and it is given as

$$q = uh = \alpha h^m \quad (2)$$

Using manning's equation,

$$m = 5/3 \text{ and } \alpha = S_o^{1/2}/n \quad (3)$$

in which  $n$  is the Manning coefficient ( $MC$ ) and  $S_o$  is the slope in the flow direction.

There is only one parameter to be defined in Eq.1 while the manning's coefficient values are available in literature (Engman, et al., 1986). The solution is obtained by using the Newton-Raphson technique. Numerical experiments are carried out to compare the performance of the four-point implicit finite difference schemes with the analytical solution of kinematic wave equations (Singh, et al., 1976). The simulations are applied to a test plane 900 m long and 1 m wide, which is subjected to a rainfall of 0.05 mm/min for 120 min. While Manning's coefficient used is  $n=0.02$  with the slope of the plane at 0.75%. In addition, simulation is ran for 300 min using a time step of 90 s and a space discretization of 30 m. The results obtained by the model are almost identical with the analytical solutions as shown in Fig. 1.

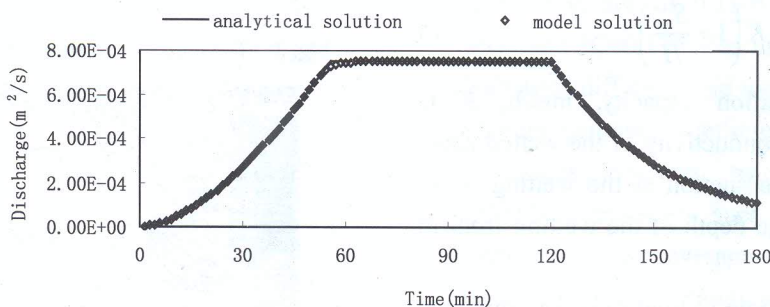


Fig. 1 Comparison of numerical and analytical solutions of kinematic wave equation

## 3 DESCRIPTION OF THE DISTRIBUTED RAINFALL-RUNOFF MODEL

The model simulates runoff yield and overland routing over a basin during storm event. The model is one-dimensional and simulates concurrently these processes: rainfall interception; through fall infiltration to the soil and overland flow routing as shown in Fig. 2.

### 3.1 RAINFALL INTERCEPTION

The interception process is simulated by a

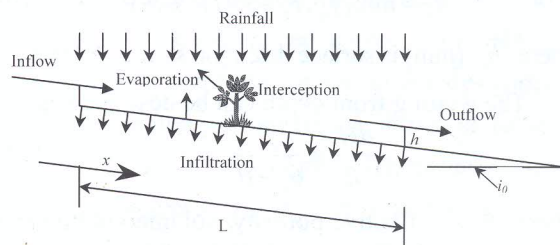


Fig. 2 A schematic of runoff generation in the model

bucket model (Kristensen, et al., 1975), where precipitation  $P$  (mm) in excess of interception storage  $INT$  (mm) and evaporation  $E$  (mm) from interception reaches the ground surface. The interception storage varies between zero and  $INTC$  (mm), the interception storage capacity, which is



calculated from

$$INTC = IC * LAI \quad (4)$$

where  $LAI$  is the dimensionless leaf area index; and  $IC$  is the interception coefficient (mm/unit LAI).

For each time increment  $[t-1, t]$ , the actual interception storage  $INT_t$  (mm) is calculated as follows:

$$INT_t = INT_{t-1} + INTP_t - E_t \quad (5)$$

with

$$E_t = \min(E_{pot}, INT_t) \quad (6)$$

and

$$INTP_t = \min(P_t, (INTC - INT_{t-1})) \quad (7)$$

where  $INTP_t$  is interception precipitation (mm);  $E_{pot}$  is potential evaporation (mm) and it is determined by the pan measured evaporation;  $E_t$  is evaporation from interception storage (mm).

### 3.2 THROUGH FALL INFILTRATION

The Green-Ampt method is used here. The basic equation is

$$f_c = K \left( 1 + \frac{S_{av}}{H} \right) \quad (8)$$

where  $f_c$  is infiltration capacity, mm/h;  $K$  is saturated hydraulic conductivity of the wetted zone, mm/h;  $S_{av}$  is average suction at the wetting front, mm;  $H$  is the average depth of the wetting front in the soil (mm).

The infiltration rate at time  $t$  can be computed as

$$f_t = \min(f_c, P_t - INTP_t + \bar{h}_t) \quad (9)$$

where  $\bar{h}_t$  (mm) is surface detention storage at time  $t$ .

The wetting front depth can be described as

$$\frac{dH}{dt} = \frac{f_t}{\theta_s - \theta_i} \quad (10)$$

where  $\theta_s$  is effective porosity, volume/volume and  $\theta_i$  is initial soil moisture content, volume/volume.

## 4 DELINEATION OF DIGITAL RIVER BASIN

### 4.1 STUDY AREA

The 5930 km<sup>2</sup> Shiguanhe basin (see in Fig. 3)

is prone to heavy rainfall events of high intensities and temporal variability. In this paper, discharge of Meishan and Nianyushan station were used as the inflow to the study area (2954 km<sup>2</sup>) between Jiangjiayi station and the two reservoirs; this is depicted as the plain light colored area in Fig. 4.

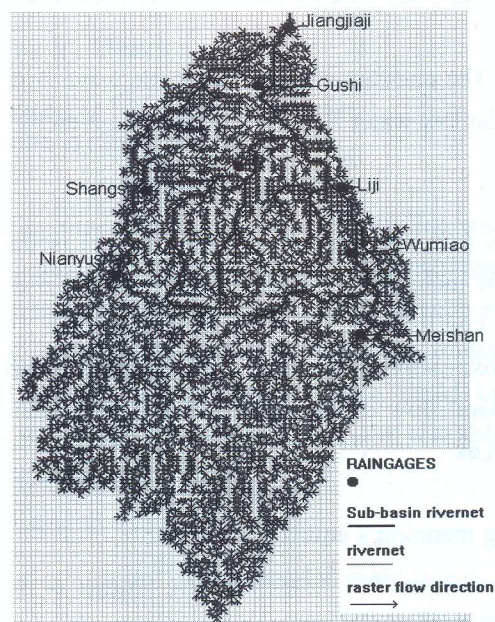


Fig. 3 The digital watershed of Shiguanhe watershed

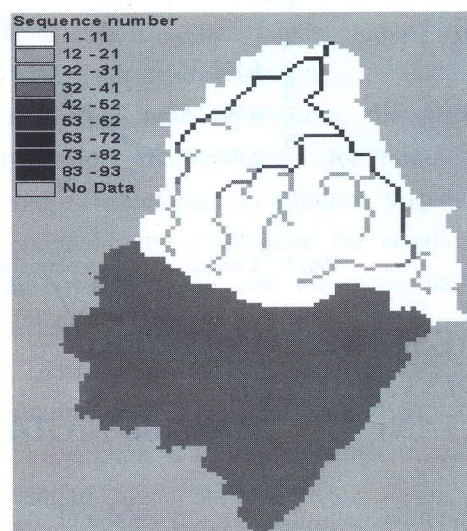


Fig. 4 Sequence number of grid

### 4.2 DIGITAL RIVER BASIN FOR SHIGUANHE RIVER

The topographic information for the basin is available from the U.S. Geological Survey's EROS Data Center in the form of a digital elevation model (GTOPO30). The digital river basin of Shiguanhe



basin with an area 5830 km<sup>2</sup> is extracted by using the DigitalHydro software package (Liu, et al., 2005). It is 1.6% less than the actual area. Raster Flow direction and slope for the raster system can also be gained. By assigning a critical upstream area, in this study basin 30 km<sup>2</sup>, the hillslope and river grids are differentiated.

The flow concentration system of the basin is routed according to this algorithm. Each cell has a routing order and the cells are ranked by the following principles: (1) cells without inflow are defined as rank 1, and (2) the ranking number of each cell is equal to the maximum ranking number among neighboring upland cells plus 1. There is no flow between cells of equal rank. According to these methods, the raster system of the study area is divided into 93 ordered areas for overland flow routing as shown in Fig. 4.

## 5 MODEL APPLICATION

### 5.1 HYDROLOGY AND CLIMATE DATA

Rainfall data from a weather radar located in Fuyang station (32° 55'N, 115° 49'E) was available. Hourly and daily average discharge data were monitored at Jiangjiaji, Meishan, Nianyushan and Huangnizhuang station and hourly and daily average rainfall were monitored at 16 locations in the basin. From 1970s to 2000s, seven flood events, five for calibration and two for validation, were selected for hydrological modeling.

### 5.2 VEGETATION AND SOIL DATA

Vegetation distribution of the catchment is obtained from the UMD 1km global land cover database. Distribution of the nine types of vegetation is shown in Fig. 5.

Soil type data is from FAO Soil Map of the World (FAO, 1998). According to the soil type data, fundamental soil properties such as depth, particle size distribution and effective porosity are from

IGBP-DIS (2000).

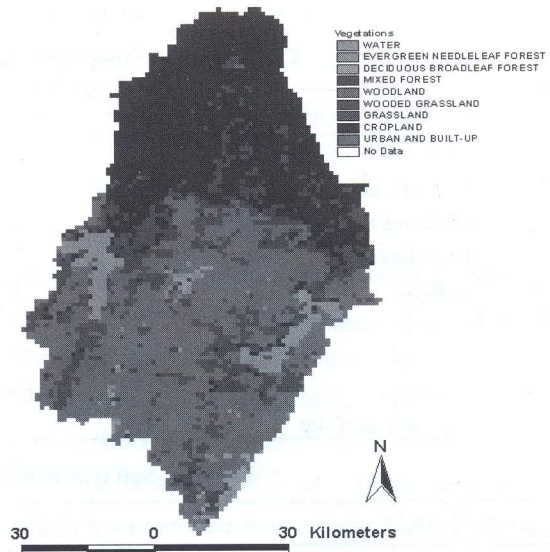


Fig. 5 Spatial distribution of vegetation type

### 5.3 CALIBRATION AND VALIDATION

The interception coefficient  $IC$  can be related to the thickness of water film on the leaves, with maximal values of 0.15-0.20mm (Menzel, et al., 1997) and  $IC=0.175$  was used for the study basin. Grids with different land use were assumed to be of different manning coefficients ( $MC$ ) according to the values measured by Engman (1986). Soil hydraulic parameters such as saturated hydraulic conductivity and average suction at the wetting front suggested by Rawls et al. (1983) were used. The manning's coefficients and soil hydraulic parameters were determined based on published literatures as introduced above with only a little adjustment according to the outlet discharge data. The calibrated parameters are shown in Table 1 and Table 2. The initial soil moisture was near saturation for the selected flood events and was consistent with actual watershed conditions.

The efficiency coefficient ( $EC$ ) used to quantify model performance is

$$EC = 1 - \frac{\sum (Q_{obs} - Q_{sim})^2}{\sum (Q_{obs} - \bar{Q}_{obs})^2} \quad (11)$$

where  $Q_{obs}$  is the observed discharge (m<sup>3</sup>/s),  $Q_{sim}$  is the simulated discharge (m<sup>3</sup>/s), and  $\bar{Q}_{obs}$  is the average value of observed discharge (m<sup>3</sup>/s). The simulation



results are listed in Table 3. All the simulated peak discharges are compatible to the observed ones and the biases are low for all flood events.

**Table 1 Vegetation type and corresponding manning's coefficients**

Vegetation type	Area (km <sup>2</sup> )	Manning coefficients	Leaf area index
Water	224	.01	0
Evergreen needle leaf forest	52	.141	6
Deciduous broad leaf forest	66	.141	6
Mixed forest	38	.193	6
Woodland	2409	.114	6
Wooded grassland	777	.102	2
Grassland	278	.102	2
Cropland	1988	.091	2
Urban and Built-up	2	0.02	0

**Table 2 Soil type and parameters for Green-Ampt model**

Soil type	K (cm/hour)	$\theta_s$ (cm <sup>3</sup> /cm <sup>3</sup> )	$S_{av}$ (cm)
Calcaric Gleysol	0.392	0.499	27.3
Eutric Gleysol	0.382	0.539	29.2
Calcic Cambisol	0.868	0.485	16.7

**Table 3 Hydrological simulation results**

	Flood events (year/month/day)	Peak discharge			Efficient coefficient
		Obs. (m <sup>3</sup> /s)	Sim. (m <sup>3</sup> /s)	Bias (%)	
Calibration	1975/06/20	2430	2632	-8.3	0.90
	1980/07/16	3020	2964	1.9	0.93
	1987/05/01	1010	846	16.2	0.85
	1998/06/28	1390	1420	-2.2	0.78
	2002/07/22	3080	2954	4.1	0.85
Validation	1987/07/05	3540	3666	-3.6	0.88
	1991/06/11	2330	1987	14.7	0.86

## 6 SUMMARY AND CONCLUSION

A grid-based kinematic wave overland flow model for digital river basin was developed and applied as a distributed hydrological model for basin scale rainfall-runoff modeling. The distributed rainfall-runoff model was applied to Shiguanhe basin, an experimental basin during the Intensified Observation Period (I.O.P.) of HUBEX in 1998/1999. The basin was sub-divided into a raster system to represent the spatial variability of rainfall field, soil vegetation and so on. The topography such as raster slope, flow vector and digital river were extracted by a digital watershed tools, DigitalHydro. Seven flood events were selected for calibrating and

validating the model. The parameters were calibrated by five flood events by referring to the values suggested by literatures. The simulated results show good agreement with the observed. The results show that this distributed rainfall-runoff model performed well as it is capable of evaluating the impacts of land cover and soil changes by human activities on the outlet discharge, so well.

## REFERENCE

- Beven, K.J., Kirkby, M.J., et al. (1984) Testing a physically based flood forecasting model (TOPMODEL) for three U.K. catchments. *J. Hydrol.* 69: 119-143.
- Liu, X.Y., Mao, J.T., et al. (2002) Radar rainfall estimation and its application to runoff simulation over Shiguanhe catchments. *J. Peking University* 38:

- 342-349 (in Chinese).
- Li, Z.J., Ge, W.Z., et al. (2004) Coupling between weather radar rainfall data and a distributed hydrological model for real-time flood forecasting. *Hydrol. Sci. J.* 49: 945-958.
- Kibler, D.F., Woolhiser, D.A. (1970) Mathematical properties of the kinematic cascade. *J. Hydrol.* 15: 131-147.
- Engman, E.T. (1986) Roughness coefficients for routing surface runoff. *J. Irrig. Drainage Eng. Am. Soc. Civ. Eng.* 112: 39-53.
- Singh, V.P., and Woolhiser, D.A. (1976) A nonlinear kinematic wave model for watershed surface runoff. *J. Hydrol.* 31: 221-243.
- Kristensen, K.J., Jensen, S.E. (1975) A model for estimating actual evapotranspiration from potential evapotranspiration. *Nordic Hydrology*, 6: 170-188.
- Liu, J.T., Feng, J. (2005) A Distributed Flow Routing Model Based on DEM and Its Application in Flood Forecasting. *Water resources and power*, 23: 11-14. (in Chinese)
- FAO. Land and water digital media series N-1, December, ISBN 92-5-104050-8, 1998.
- Global Soil Data Task. Global Soil Data Products CD-ROM (IGBP-DIS). Available online at [<http://www.daac.ornl.gov/>] from the ORNL Distributed Active Archive Center, Oak Ridge National Laboratory, Oak Ridge, Tennessee, U.S.A., 2000.
- Menzel, L. (1997) Modellierung der evapotranspiration im system Bodem-Pflanze-Atmosphäre. *Zurcher Geographische Schriften*, Band 67, Geographisches Institut, Eidgenossische Technische Hochschule, Zurich, Switzerland, 128pp.
- Rawls, W. J., Brakensiek, et al. (1983) Green-Ampt infiltration parameters from soil data. *J. Hydr. Engrg., ASCE* 109: 62-70.